

# Research article

## Morphology and elemental analysis of freshly emitted particles from packed-bed domestic coal combustion

Masilu Daniel Masekameni<sup>1\*</sup>, Tafadzwa Makonese<sup>3</sup>, Isaac Tebogo Rampedi<sup>2</sup>,  
Goitsewang Salvation Keretsetse<sup>1</sup>

<sup>1</sup>Occupational Health Division, School of Public Health, Faculty of Health Sciences, University of the Witwatersrand, South Africa

<sup>2</sup>Department of Geography, Environmental Management and Energy Studies, University of Johannesburg, Johannesburg, South Africa

<sup>3</sup>Process, Energy & Environmental Technology Station, Faculty of Engineering and the Built Environment, University of Johannesburg, Johannesburg, South Africa

\*Correspondence: [daniel.masekameni@wits.ac.za](mailto:daniel.masekameni@wits.ac.za)

Received: 18 July 2020 - Reviewed: 1 September 2020 - Accepted: 30 November 2020

<https://doi.org/10.17159/caj/2020/30/2.8582>

### Abstract

This study was conducted in a laboratory-controlled environment to analyse the physical properties and elemental composition of coal combustion particles in a brazier. Particles were sampled ~1 m above the stove, using a partector. Particles were collected on gold transmission electron microscopy (TEM) grids, and polycarbonate filters for TEM and inductively coupled plasma mass spectrometry (ICP-MS) analysis, respectively. Particles for elemental analysis were collected on a 37 µm polycarbonate filter, and the exhaust was drawn in using a GilAir Plus pump. During sampling, a 2.5 µm cyclone was attached to the sampling cassette to isolate larger particles. Combustion particles emitted during the early stage of combustion were single organic spherical particles with similar characteristics to tarballs. As the combustion progressed, the particle diameter gradually decreased (from 109 nm), and the morphology changed to smaller particles (to 34.3 nm). The particles formed accretion chain structures, showing evidence of agglomeration. Furthermore, a fluffy microstructure, resembling the formation of soot, was formed in the post flaming phase. In the char-burning phase, an irregular structure of semi-spherical particles was formed, showing evidence of mineral particles infused with small carbonaceous particles. Similarly, with the findings of previous studies, the present research also observed organic spherical particles similar to tarballs. Given that during the ignition phase there was a simultaneous burning of wood as kindling and coal, the provenance of these particle emissions can be attributed to both coal and wood.

### Keywords

physical properties, D-grade coal, brazier, transmission electron microscopy, inductively coupled mass spectrometry, elemental composition

### Introduction

Despite efforts to reduce dependence on solid fuel, more than 3 billion people continue to burn coal and wood for cooking and space heating (Naeher et al., 2007; Gordon et al., 2014). Small diameter (< 2.5 µm) particulate matter has been singled out as posing a significant threat to both the environment and human health. Suspension of fine particles has been associated with household emissions from wood and coal burning (McDonald and Biswas, 2004; Chafe et al., 2015).

Several epidemiological studies have shown that particles below PM<sub>2.5</sub> are strongly associated with infection of the lower respiratory tract, cardiovascular system disruption, and morbidity (Lim et al., 2012, 2013). Despite severe health

effects, the source to exposure mechanisms from domestic coal and wood-burning has not yet been established. Researchers recommend that an understanding of particle evolution from its point of release to the microenvironment of the receptor is important for source and hazard mapping (Shen et al., 2013; Torvela et al., 2014). Therefore, the correct determination of the physicochemical properties of coal/ wood emissions particles is essential for source identification and characterisation. However, very few studies have been conducted on the physicochemical properties of particles emitted from small scale coal combustion technologies, even though significant associated health risks have been reported in countries such as China, India and Finland (Niemi et al., 2006; Wilkinson et al., 2009; Zhang and Tao, 2009).

Characterisation of the organic fractions emitted from domestic coal-burning technologies has been reported globally (Bazilian et al., 2012; Zhang et al., 2012). However, very few studies have focused on the characterisation of trace elements emitted from residential coal burning (Bazilian et al., 2012; Silva et al., 2012). Studies conducted in China have reported possible health effects of trace elements emitted from residential coal burning (Smith et al., 2014; Zhang, Zou, et al., 2018). In 2004 it was reported that, in Guizhou province, more than 3 000 people had suffered arsenic poisoning, bone deformation, human selenosis and fluorosis because of exposure to residential coal burning (Finkelman, 2004; Zhou et al., 2015). Furthermore, it was established that the health effects of trace elements from coal-burning vary according to the properties of the coal, and exposure scenarios (Masekameni, Makonese and Annegarn, 2014; Zhang, Zou, et al., 2018). In South Africa, especially in the central plateau of the Highveld region, coal burning, using unvented stoves, continues to be a significant source of energy for domestic cooking and heating (Balmer, 2007; Makonese et al., 2017). Efforts to reduce dependence on coal at the domestic level in South Africa have been commissioned, although they have not yet been fully implemented (Bonjour et al., 2013; GroundWork, 2016).

Household air pollution inventories in South Africa are limited due to inadequate data from source apportionment studies. Only a few studies used scanning electron microscopy (SEM) to confirm the physical properties of particles emitted from domestic coal and wood burning. Nevertheless, data generated from SEM analysis are not sufficient for source apportionment. Contrary to SEM, transmission electron microscopy (TEM) analysis is considered to provide a better characterisation of the internal structures of particles and is the preferred method for studying the shape and morphology of aerosol particles (Schneider et al., 2006; Gwaze, 2007).

Equipped with energy dispersive X-ray (EDX) or electron energy loss (ELL) spectroscopy, the instruments provide information about the elemental composition of the analysed particles (Nussbaumer et al., 2001). For TEM, very thin grids (often copper/gold), coated with a carbon or gold film are used. The quality of the film is essential to obtain good resolution (Mathis et al., 2005). If samples are used for quantitative analysis (e.g. the size distribution), care must be taken to have defined size fractions during the sampling process (Nussbaumer et al., 2001; Bond et al., 2006). In addition to particle morphology, the correct identification and determination of the elemental composition rely on the use of effective analytical techniques. Inductively coupled mass spectrometry (ICP-MS) has been widely used to study the elemental composition of combustion particles. In this study, we analysed the physical properties and selected elemental composition (Na, Mg, Al, Si, K, Ca, Ti, V, Cr, Mn, Fe, Co, Ni, Cu, Zn) of particles generated during residential coal burning during three combustion phases (ignition, flaming and coking).

Currently, in South Africa, several studies on emissions from industries are underway, but there are limited studies to

apportion the contribution of domestic coal/wood burning to air pollution. Our study aimed to examine the morphology and chemical analysis of particles emitted during the combustion of D-grade coal, during three combustion phases (ignition, flaming and char burning), to determine the source contribution of particulate matter and to further our understanding of pollutant source distribution.

We used lumps of D-grade type coal that were burned in a high-ventilated stove and lit with a top-lit updraft (TLUD) ignition method in three combustion phases (ignition, flaming and char burning). The limitation of D-grade coal was fostered, as it is the most common fuel available in the informal settlements and townships of South Africa. D-grade coal is considered poor quality coal with ash content of over 14%, carbon content of 55% and volatiles at about 25%.

## Materials and methods

### Experimental stove and fuel analysis

D-grade coal was burned in a high-ventilated stove lit using a Top-lit Updraft (TLUD) ignition method in a laboratory-controlled environment. Particles emitted during three combustion phases (ignition, flaming and char burning) were analysed. Due to variations of field-based factors, several variables were kept constant (i.e. ventilation rates, the position of the fuel grate inside the stove, size of coal lumps, ignition method and kindling fuel). The stove characteristics are shown in Figure 1.

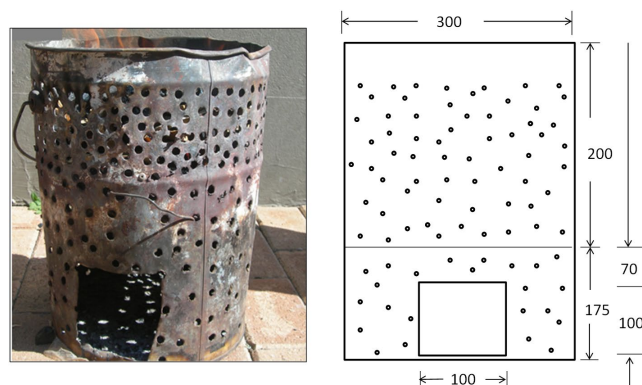


**Figure 1:** A photograph and schematic representation of a high ventilation field purchased brazier stove used in the experiments (Not drawn to scale – dimensions are in mm).

Coal particle size was determined by sieving the coal using a 40 mm x 60 mm diameter mesh. The coal was analysed by Bureau Veritas Inspectorate Laboratories (Pty) Ltd., using the standard methods. Experimental results are based on the proximate and ultimate air-dried D-grade coal analyses (Table 1).

During the TLUD ignition method, 2 500 g of coal were placed on the grate, followed by 35 g of paper, 400 g of wood kindling, and another 1 500 g of coal. Details on the division of the combustion phases, fuel properties and ignition method are detailed in a previous paper (Masekameni et al., 2018).

**Table 1:** Proximate and ultimate analysis values for the coal (merchants and colliery) on an air-dried basis

Parameter (air-dried basis)	Standard method	Slater mine D-grade coal
Moisture content (%)	ISO 5925	1.8
Volatiles (%)	ISO 562	20.3
Ash (%)	ISO 1171	24.2
Fixed carbon (%)	By difference	57.5
Calorific value (MJ kg <sup>-1</sup> )	ISO 1928	23.4
Calorific value (Kcal kg <sup>-1</sup> )	ISO 1928	5590
Total sulphur (%)	ASTM D4239	0.63
Carbon (%)	ASTM D5373	62.6
Hydrogen (%)	ASTM D5373	2.76
Nitrogen (%)	ASTM D5373	1.0
Oxygen (%)	By difference	5.0
Total silica as SiO <sub>2</sub> (%)	ASTM D4326	58.6
Aluminium as Al <sub>2</sub> O <sub>3</sub> (%)	ASTM D4326	27.6
Total iron as Fe <sub>2</sub> O <sub>3</sub> (%)	ASTM D4326	6.63
Titanium as TiO <sub>2</sub> (%)	ASTM D4326	0.82
Phosphorous as P <sub>2</sub> O <sub>5</sub> (%)	ASTM D4326	0.55
Calcium as CaO (%)	ASTM D4326	2.30
Magnesium as MgO (%)	ASTM D4326	0.83
Sodium as Na <sub>2</sub> O (%)	ASTM D4326	0.42
Potassium as K <sub>2</sub> O (%)	ASTM D4326	0.79
Sulphur as SO <sub>3</sub> (%)	ASTM D4326	1.10
Manganese as MnO <sub>2</sub> (%)	ASTM D4326	0.12

## Particle sampling

Particles were collected on TEM gold grids and polycarbonate membrane filters, for TEM and ICP-MS analyses, respectively. The gold grids were placed on a grid holder from the partector aerosol dosimeter TEM sampler (Naneos particle solutions, Switzerland), and the particles were deposited directly onto the grid. The sampling train included a Teflon tube, connecting the partector inlet to the sampling cassette that was fitted with a 2.5 µm cyclone, with a PM4 cutoff point at 50%. The partector was set at a flow rate of 2.8 L/minute, according to the cyclone's specification. Sampling for inductively coupled plasma Mass spectrometry (ICP-MS) was done using polycarbonate membrane filters (37 mm diameter). The exhaust was drawn onto the membrane filter inside a cassette, using a GilAir Plus pump (Model) set at a flow rate of 2.2 L/minute. The filters were changed at the start of each combustion phase (ignition, flaming and char burning/coking).

### Preparation of filters

A total of 12 (four samples for each combustion phase), 37 mm diameter polycarbonate membrane filters, with a pore size of 0.08 µm, were stored in a controlled laboratory environment before sampling campaign. The temperature ranged from 22 – 23 °C and the humidity was recorded as 35 %. The filters were conditioned for 24 hours and pre-weighed, using a Sartorius

electronic microbalance (model CPA225D, supplied with a balance pan) with a minimum resolution of 0.001 mg and a precision of 0.001 mg. The same procedure was repeated after a three-hour burn sequence of sampling particulate matter was completed. A field blank was handled in the same way as the field filter. However, the field blank was not exposed to the particulate matter. The objective of using a field blank is to overcome or account for moisture loss due to meteorological conditions, particularly during transportation and contamination when handling the filters. The determination of the final mass was calculated using equation 1.

$$\text{Final mass} = \text{Field filter (post-pre)} + \text{field blank (post-pre)} \quad (1)$$

where the field filter (post) mass is the mass collected from the filter after sampling while the field pre-mass is the mass recorded before sampling. The field blank 'post' and 'pre' are the masses recorded after and before transportation of the filters, respectively.

### Inductively coupled mass spectrometry

The sample filters for ICP-MS analysis were folded and placed inside pre-cleaned microwave digestion vessels; about 9 mL supra pure (Merc) nitric acid (HNO<sub>3</sub>) and 1 mL supra pure (Merc) hydrogen peroxide (H<sub>2</sub>O<sub>2</sub>) were added to each vessel. A reagent blank was included with the batch as a control. The vessels were closed and placed in a Mars 6 microwave. The digestion method made the vessels ramp to 200 °C for 20 minutes, and hold the temperature for another 15 minutes. The samples were then quantitatively transferred to 50 mL volumetric flasks and made up to the mark using 18.2 M Ω /cm ultrapure water. Calibration standards of 0 µg/L, 0.1 µg/L, 0.5 µg/L, 1.0 µg/L, 5.0 µg/L and 10 µg/L were prepared from 100 mg/L NIST traceable stock standards. The samples were then filtered using a 0.45 µm syringe filter and diluted 10 times (1 ml diluted to 10 ml) before analysis by ICP-MS. The blank filter analysis, using the ICP-MS technique, was carried out in the same manner as the sample filters. Since our samples were mostly carbon from a combustion process, we did not use hydrogen fluoride (HF) which is often used in dissolving samples of non-carbonaceous nature. For quality assurance, the instruments were optimized with a tune solution before analysis and calibrated with NIST traceable standards.

In this study, we noted that ICP-MS is a sensitive technique and that caution should be exercised when analysing samples. Many sources can contribute to the overall accuracy and precision of the analysis. Therefore, internal standards with a mass number close to that of the analyte element(s) were used to minimise errors inherent in the analytical method. The internal standards assist to correct for matrix differences between calibration standards and samples. Since samples can easily suffer from Easy Ionizable Elements (EIE) effect, the loss of ionization efficiency can be corrected. Moreover, imprecision arising from small variations in dilutions can also be corrected. The correction procedure followed in this study is similar to that detailed in Vanhaecke et al. (1992).

### Transmission electron microscopy (TEM)

Combustion smoke particles were imaged for their morphologies, using JEM-2100, in a multipurpose, 200 kV analytical electron microscope, at the University of Johannesburg, South Africa (Jeol Ltd from Akishima, Tokyo, Japan, manufactures the instrument). TEM has been used to study the semi-structure especially respirable particles, in contrast to optical microscopy, which uses light as an illumination source for imaging. TEM uses electrons which provide an opportunity to separate arrangements of atoms in small structure/ combustion soot aggregates (Kocbach et al., 2005; Wang et al., 2018). TEM combines the JEM-2100 optic system with an advanced control system for ease of operation.

### Physical properties of coal emissions

In an earlier study, Masekamani et al. (2018) reported physical properties of coal emissions particles for similar combustion activities. Particle size distribution (PSD) of around 109 nm, 54 nm and 31 nm for the ignition, flaming and coking phase were reported respectively (Table 2). The particle morphology shown by Masekamani et al. (2018), suggests that particle diameter was larger at the ignition phase and gradually decreased as the combustion process progressed.

**Table 2:** PSD of coal emission particles in a brazier

Phase	Duration (minutes)	GMD (nm)	GSD (nm)
Entire Combustion Sequence	180	51.9	2.1
Ignition	20	109.8	18.4
Flaming	60	54.9	5.9
Coking	100	34.3	5,1

## Results and discussion

### Morphology of coal particles from TEM analysis

#### Morphology of smoke particles emitted during the ignition phase

The morphology of particles observed using a TEM for the ignition phase shows giant single spherical particles. Moreover, we used TEM analysis to study and distinguish different smoke particle morphologies similar to previously conducted studies (Pósfai et al., 2004; Chakrabarty et al., 2010; Tóth et al., 2014a). Figure 2 shows the morphology of smoke particles emitted during the ignition phase of coal combustion.

Figure 2a shows a spherical organic particle, with the characteristics of tarballs, collected from low-temperature combustion during the ignition phase. Emission of spherical organic particles is synonymous with smouldering combustion conditions. This suggests that the spherical particles are emitted because of low-temperature combustion. Posfai et al. (2003) contended that these carbonaceous particles are formed in smouldering fires and that they increase in abundance in the atmosphere as the smoke plume ages.

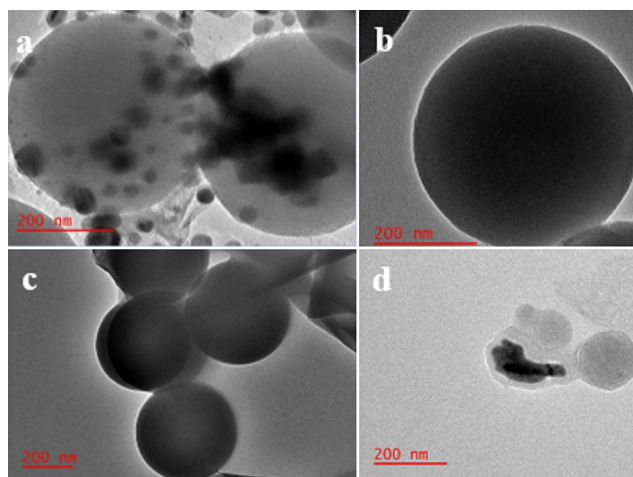


**Figure 2:** TEM images of particles emitted during the ignition phase of coal combustion. a) carbonaceous spherical particle, b) internal structure of spherules with evidence of aggregates, c) onion-like structured soot particles, d) single-particle exposed to high beam resolution.

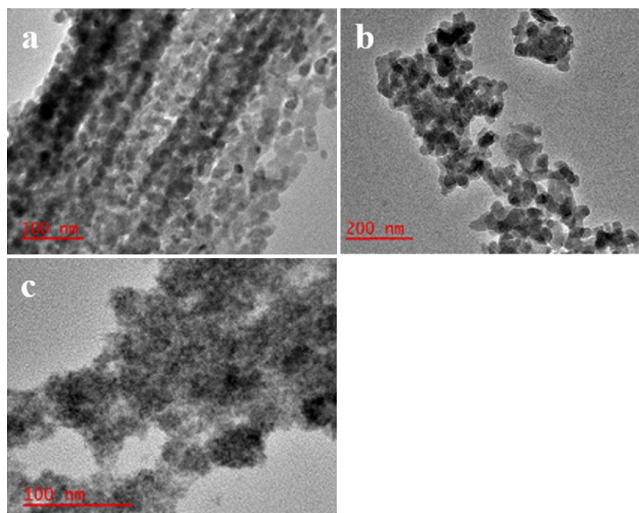
Furthermore, Posfai et al. (2004) reported similar morphologies to the ones reported in this study. However, the source contribution in their study was veld fires, which are often dominated by biomass burning. Figure 2b shows large organic spherical particles infused with diffusion accretion chains, forming soot. It was observed that, since these particles were collected at 1 m above the stove, the morphology might change with an increase in the height of sampling due to ageing of the particles.

Figure 2c shows particle growth as the spherical organic particles fuse, probably due to collision. Thajudeen et al. (2015) suggested that particle-particle collision is the dominant particle growth mechanism during combustion, even though the particles may restructure or rearrange after the collision and fail to coalesce. Particles with similar morphologies to those found in our study were observed from biomass burning fires (Shraim et al., 2003; Thajudeen, Jeon and Hogan, 2015). Figure 2d shows the onion-like structure of emitted organic particles, with disordered graphic layers, observed in the high-resolution TEM image.

Spherical organic particles shown in Figure 2 indicate a homogeneous structure (spherical), showing darker and lighter areas under TEM. The spherical organic particles have properties similar to tarballs produced during biomass burning. Similar morphologies were observed in previous studies (Pósfai et al., 2003; Tóth et al., 2014a). However, the literature suggests that tarballs are only released as a consequence of smouldering wood-burning fires. Several scholars have reported that tarballs are not emitted during coal or oil combustion (Pósfai et al., 2003; Tissari et al., 2008; Tóth et al., 2014b, 2014a).

#### Morphology of coal particles emitted during the flaming phase

During the flaming phase, particle diameter (54.9) was smaller than that during the ignition phase (Figure 3a, 3b and 3c). The



**Figure 3:** TEM images of carbonaceous particles emitted during the flaming phase- a) carbonaceous soot particles showing as aggregates, b) a more established and well-arranged accretion chain, c) fluffy microstructure, resembling soot particles, d) single-particle exposed to high beam resolution.

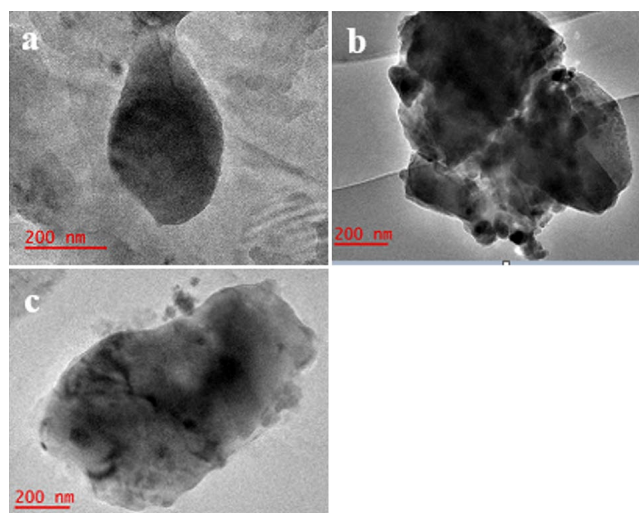


**Figure 4:** TEM images of particles emitted during the char burning phase- a) irregular structure of semi-spherical particles, b) mineral particles infused with small carbonaceous particles, c) a fully established macro-structure, indicating the presence of non-water soluble compounds.

formation of the spherical particles during ignition is thought to be influenced by the release of polar compounds from smouldering fires. During flaming, fewer polar compounds, which affect particle growth, are emitted than during the ignition stage (Pósfai et al., 2004). The particles observed, using TEM, resemble fused small particles with diffusion accretion chains that have characteristics similar to soot (Figure 3 a, b and c). Soot contains aggregates of small particles often less than 60 nm in the diameter. A morphology similar to the present study was reported from a study in Guizhou Province, China (Shraim et al., 2003). However, the researchers who conducted that study investigated the morphology of particles in ageing smoke, from a wood fire. It is important to note that, in the study reported in this paper, the images were obtained from freshly produced particles. A well-arranged morphology, consisting of single

particles, can be seen in figure 3b. Other researchers have also reported that the particle diameter decreases as the combustion conditions progress (Niemi et al., 2006).

Shraim et al. (2003) and Posfai et al. (2004) reported that there was an increase on the number of tar balls in samples collected at further distances from the emitting source, suggesting that there was particle growth because of condensation of organic gases, or transformation due to collision with other organic atmospheric particles. In our study, we have shown a mechanism to which particles transform as the combustion progresses (Figure 3c). We established that, as coal heats up, it swells and cracks. It is through these cracks that organic particles are released and, depending on the ignition method and combustion conditions, a brown to thick white plume is evident, which may pass through a cold zone above the burning coal into the ambient air. We previously demonstrated that, as combustion progresses, fine particles, often enriched with low volatile organic gases, are emitted (Masekameni et al., 2018). Furthermore, particle growth is as a result of the water injection in the coal and which is released as water vapour during coal pyrolysis (Chang et al., 2004). Therefore, accretion chains may be caused by coagulation of particles emitted during the flaming phase (Makonese, 2015; Makonese, Masekameni and Annegarn, 2017). As the coal fully pyrolyze, fluffy microstructures are formed, which have the same characteristics as soot particles.

In summary, the findings from our study build on the work of Makonese (2015) and Toth et al. (2014b), who recommended that further studies be conducted to affirm the existence of spherical organic particles, tarballs and related particle formation mechanisms in domestic combustion processes. We confirm that spherical organic particles with similar characteristics to tarballs are emitted as a consequence of smouldering combustion conditions. In this study, we have demonstrated that residential coal burning may be a source of - spherical organic particle-like tarball emissions. However, since wood kindling was used during the ignition phase, it might be that some of the emissions of the spherical organic particles similar to tarballs could have been released from the simultaneous combustion of wood kindling and coal.

### Morphology of coal particles emitted during the char burning phase

Figure 4 shows images of particles collected during the char burning stage of coal-combustion, in a typical brazier used in South African informal settlements. During the char-burning phase, almost all volatile organic compounds have been released during the ignition and flaming phases (Masekameni et al., 2018). This results in the emission of non-carbonaceous matter during the coking phase, usually in the form of mineral particles from the burning char (Figure 4 a, b and c). In this stage, the fire burns uniformly if there is sufficient oxygen supply, and particles emitted during this stage are similar to those particles reported in studies of ash. The mineral particles are irregular in shape and tend to have a much smaller diameter (34.3 nm) than soot and homogeneous spherical organic particles (Figure 4a).

In Figure 4b, a closer look on the mineral particle indicates that there are several smaller particles of irregular shapes fused or agglomerated. Existing literature recognizes these particles as being composed of several mineral elements, including Si, Ca, Al, Fe, Na, K, Mg, and P (Wang and Luo, 2009). In Figure 4c, a mineral enriched irregular particle was imaged under the TEM. This particle is different from particles shown for the ignition and flaming phases, respectively.

This study did not employ EDX to determine the composition of each mineral particle semi-quantitatively. It is recommended that further studies be carried out to determine the elemental composition of specific mineral particles emitted during the char burning stage of domestic fixed-bed coal combustion. This study has employed ICP-MS to ascertain the elemental contribution of each combustion stage to the overall emissions of elements across the entire burn cycle sequence.

### Elemental analysis of coal combustion particles during the ignition, flaming and char burning phases

Table 3 lists the ICP-MS results of selected trace elements collected during the three combustion phases (ignition, flaming, and char/coking burning), and across the entire burn cycle. During the ignition phase, Ca, Si, Fe and K were released in the highest proportions. The elemental composition derived from the total PM is expressed in mg, while the total trace elements are expressed in µg as shown in Table 3 and Table 5. These results, especially the emission of Si and K, suggest a particle partitioning, similar to that shown in previous studies (Hand et al., 2005; Meij and te Winkel, 2007; Zhang, Liu, et al., 2018). The smoke particles with high Si content can be used as a marker for coal combustion emissions, while the smoke particles with a high K percentage suggest emissions from biomass burning (in this case, wood kindling was used during the ignition phase).

During the ignition phase, the percentages of both Si and K were high because wood fuel was used as kindling to ignite the coal nuggets. In the flaming phase, the percentage contribution of K was higher than in the ignition and char burning phases. The increase in the percentage of K during flaming is possibly due to the pyrolysis of the wood kindling. A noticeable decline in the percentage of potassium can be seen during the char burning phase. For the marker of coal emissions, a relatively steady increase in Si emission confirms that the particles are from

coal combustion. All trace element emissions, except Ca and K, steadily increased as the combustion progressed. K and Ca emissions are thought to be associated with the pyrolysis wood kindling which often completes in the second half of the flaming stage (Makonese et al., 2014).

In previous studies, the elemental composition of emissions from coal-burning boilers/ furnaces was limited to fly ash, with little emphasis on the elemental composition of smoke emissions from the different combustion phases (McElroy et al., 1982; Petaloti et al., 2006). Particles emitted during the coking phase are enriched with volatile organic trace elements categorized as class one (i.e. Al, Ca, Ce, Cs, Eu, Fe, Hf, K, La, Mg, Sc, Sm, Si, Sr, Th and Ti) and are comparable to emissions in ash. During coal combustion, the minerals in the coal are deposited as bottom ash, and some are given off as fly ash (Lu et al., 2017). The types of mineral elements released are related to the mineral content of the fuel (Table 4).

A comparison of the composition of the fuel burned with corresponding elements is provided in Table 4. Although there was a relatively low amount of K in the coal, the emitted particles contained K. This was expected as wood was used as kindling to ignite the coal. The results reported in this study on trace elements are similar to those described for emissions of ash in other studies (Makonese, Meyer and Solms, 2019).

Table 5 shows the percentage and mass concentration of trace element composition of particles emitted during the three combustion phases. With decreasing volatile matter from the burning fuel, mineral particles dominated the char burning phase. The mass of the trace elements emitted during the char burning phase was 3 times higher than that emitted during the ignition phase, and twice that emitted during the flaming phase. As expected, the bulk of the elements was emitted during the char burning phase relative to the flaming and ignition phases (Zhang, Liu, et al., 2018). This finding suggests that the majority of particles emitted during the ignition and flaming phases could be dominated by volatile organic compounds (Zhou et al., 2016). During the char-burning phase, most non-water-soluble trace elements are expected to be released.

**Table 3:** Elemental composition results from inductively coupled plasma mass spectrometry (ICP-MS) analysis

Combustion phase	Element (µg/g)														
	Na	Mg	Al	Si	K	Ca	Ti	V	Cr	Mn	Fe	Co	Ni	Cu	Zn
Ignition (µg/g)	0.8	0.2	0.2	2.3	1.4	3.9	0.1	0.0	0.1	0.0	0.8	0.0	0.1	0.0	0.2
% contribution	8.3	2.3	2.0	22.5	13.8	38.4	0.7	0.0	1.4	0.2	7.5	0.1	0.5	0.1	2.2
Flaming (µg/g)	0.9	0.4	2.0	3.8	3.2	1.6	0.1	0.0	0.3	0.1	2.6	0.0	0.0	0.0	1.1
% contribution	5.3	2.7	12.5	23.3	20.0	9.9	0.9	0.0	1.6	0.4	16.0	0.1	0.1	0.2	7.0
Char burning (µg/g)	1.3	1.0	6.3	8.1	4.8	2.3	0.4	0.0	0.2	0.2	5.7	0.0	0.0	0.1	1.7
% contribution	4.1	3.1	19.7	25.3	14.9	7.3	1.1	0.0	0.6	0.5	17.9	0.0	0.1	0.2	5.3

**Table 4:** Comparison of trace elemental composition of fuel and particles emitted during the overall combustion process

Coal Analysis Results			
Element	% Contribution	Standard Method	% Contribution
Si	23.7	ASTM D4326	58.6
Al	11.4	ASTM D4326	27.6
Fe	13.8	ASTM D4326	6.6
Ti	0.9	ASTM D4326	0.8
Cr	1.2	ASTM D4326	0.6
Ca	18.5	ASTM D4326	2.3
Mg	2.7	ASTM D4326	0.8
Na	5.9	ASTM D4326	0.4
K	16.2	ASTM D4326	0.8
S	1.1	ASTM D4326	1.1
Mn	0.4	ASTM D4326	0.1

**Table 5:** Percentage contribution of detected elements emitted per combustion phase

Combustion phase	Total trace elements ( $\mu\text{g/g}$ )	% Contribution
Ignition	10.1	17
Flaming	16.2	28
Char burning	31.9	55
<b>Sum</b>	<b>58.2</b>	<b>100</b>

## Conclusion

This study was conducted to examine the morphology and elemental characteristics of freshly emitted individual particles emitted during three distinct combustion phases in domestic packed-bed coal. Three types of particles were classified viz., spherical organic particles with characteristics similar to tarballs, soot particles, and mineral particles. Spherical organic compounds were predominant in the ignition stage due to smouldering combustion conditions, while soot particles dominated the flaming stage. The identification of spherical organic particles is essential to understand how particles evolve once released into the atmosphere. Spherical organic compounds have been previously reported in smouldering wood-burning fires (Makonese, Meyer and von Solms, 2019). This finding brings new knowledge, suggesting that organic spherical particles may also be released during coal smouldering combustion conditions. This was demonstrated in a study conducted by Makonese et al. (2019) where coal was ignited using burning coal embers instead of wood kindling. As wood was used as kindling in this study, some of the emissions of organic spherical particles resembling tarballs could have been released from the wood fuel.

Mineral particles were predominant in the char burning stage where > 55% of the elements were released, suggesting that the combustion conditions were taking place at sufficient oxygen and temperature resulting in almost all volatiles being

completely given off and burned. Elemental composition analysis showed that the particles were rich in Si, K, Al, Fe, Ca, Zn, Na, Mg, and Ti, depending on the combustion phase. The type of mineral elements released was related to the mineral content of the fuel.

This information is essential for updating emission inventory sources, understanding radiation forcing potential, and providing a basis for warming estimation. In addition to information about the morphology of the emitted particles, the information on trace elements may be useful in source identification due to chemical signatures or emission markers. Both Si and K were high during the ignition phase indicating simultaneous combustion of wood kindling and coal. For the marker of coal emissions, a relatively steady increase in Si emission was confirmed across the entire combustion sequence indicating that the particles were emitted from coal combustion instead of wood. Further studies should be conducted to describe the morphology of emitted particles at distances further from the source.

## Acknowledgement

Sincere appreciation goes to Mr Shalala Mgwambani and Mr Kevin Kasangana for their assistance during laboratory experiments, to Mr Siyasanga Mpelane for assisting with TEM analysis, and to Mr Philip Pieterse for assisting with ICP-MS analysis. Many thanks to Professor Gill Nelson for her excellent language editing skills and moral support provided in completing this work. The article is published as a non-peer reviewed as preprints by the Atmospheric Science Journal on the 29th of November 2019. doi: 10.20944/preprints201911.0363.v1.

## Author contributions

Daniel Masekameni conceptualized and prepared the manuscript. He also experimented and wrote the first draft of the paper. Tafadzwa Makonese developed the methodology for coal emission capturing and analysis. He further supervised the sampling of particulate matter, data analysis, interpretation, and the presentation of arguments, and assisted in the editing of the manuscript. Isaac Rampedi assisted with the manuscript structure and write-up. Goitsemang Keretsetse edited the manuscript and validated methodology for elemental analysis. She further worked on aligning the manuscript to the journal style.

## References

- Balmer, M. (2007) 'Household coal use in an urban township in South Africa', *Journal Of Energy In Southern Africa*, 18(3), pp. 27-32. Available at: <http://www.erc.uct.ac.za/jesa/volume18/18-3jesa-balmer2.pdf>. <https://doi.org/10.17159/2413-3051/2007/v18i3a3382>
- Bazilian, M. et al. (2012) 'Energy access scenarios to 2030 for the power sector in sub-Saharan Africa', *Utilities Policy*. Elsevier Ltd, 20(1), pp. 1-16. <https://doi.org/10.1016/j.jup.2011.11.002>

- Bond, T. C. et al. (2006) 'Emission Factors and Real-Time Optical Properties of Particles Emitted from Traditional Wood Burning Cookstoves', *Environ. Sci. Technol.*, 40(21), pp. 6750-6757. <https://doi.org/10.1021/es052080i>
- Bonjour, S. et al. (2013) 'Solid fuel use for household cooking: Country and regional estimates for 1980-2010', *Environmental Health Perspectives*, 121(7), pp. 784-790. <https://doi.org/10.1289/ehp.1205987>
- Chafe, Z. A. et al. (2015) 'Household cooking with solid fuels contributes to ambient PM<sub>2.5</sub> air pollution and the burden of disease', *Environmental Health Perspectives*, 122(12). <https://doi.org/10.1289/ehp.1206340>
- Chakrabarty, R. K. et al. (2010) 'Brown carbon in tar balls from smoldering biomass combustion', *Atmospheric Chemistry and Physics*, 10(13), pp. 6363-6370. <https://doi.org/10.5194/acp-10-6363-2010>
- Chang, M. C. O. et al. (2004) 'Measurement of ultrafine particle size distributions from coal-, oil-, and gas-fired stationary combustion sources', *Journal of the Air and Waste Management Association*, 54(12), pp. 1494-1505. <https://doi.org/10.1080/10473289.2004.10471010>
- Finkelman, R. B. (2004) 'Potential health impacts of burning coal beds and waste banks', *International Journal of Coal Geology*, 59(1-2), pp. 19-24. <https://doi.org/10.1016/j.coal.2003.11.002>
- Gordon, S. et al. (2014) 'Respiratory risks from household air pollution in low and middle-income countries', *Lancet Respiratory Medical*, 2(10), pp. 823-860. doi: 10.1016/S2213-2600(14)70168-7. [https://doi.org/10.1016/S2213-2600\(14\)70168-7](https://doi.org/10.1016/S2213-2600(14)70168-7)
- GroundWork (2016) *The Destruction of the Highveld: Digging Coal*.
- Gwaze, P. (2007) 'Physical and Chemical Properties of Aerosol Particles in The Troposphere: An Approach from Microscopy Methods'.
- Hand, J. L. et al. (2005) 'Optical, physical, and chemical properties of tar balls observed during the Yosemite Aerosol Characterization Study', *Journal of Geophysical Research Atmospheres*, 110(21), pp. 1-14. <https://doi.org/10.1029/2004JD005728>
- Kocbach, A. et al. (2005) 'Analytical electron microscopy of combustion particles: A comparison of vehicle exhaust and residential wood smoke', *Science of the Total Environment*, 346(1-3), pp. 231-243. <https://doi.org/10.1016/j.scitotenv.2004.10.025>
- Lim, J. et al. (2013) 'a Rights-Based Approach To Indoor Air Pollution', *Health and Human Rights*, 15(2), pp. 160-167.
- Lim, S. S. et al. (2012) 'A comparative risk assessment of burden of disease and injury attributable to 67 risk factors and risk factor clusters in 21 regions, 1990-2010: A systematic analysis for the Global Burden of Disease Study 2010', *The Lancet*, 380(9859), pp. 2224-2260. [https://doi.org/10.1016/S0140-6736\(12\)61766-8](https://doi.org/10.1016/S0140-6736(12)61766-8)
- Lu, S. et al. (2017) 'Single-particle aerosol mass spectrometry of coal combustion particles associated with high lung cancer rates in Xuanwei and Fuyuan, China', *Chemosphere*. Elsevier Ltd, 186, pp. 278-286. <https://doi.org/10.1016/j.chemosphere.2017.07.161>
- Makonese, T. et al. (2014) 'Aerosol particle morphology of residential coal combustion smoke', 24(2), pp. 24-28. <https://doi.org/10.17159/caj/2014/24/2.7064>
- Makonese, T. (2015) 'Systematic investigation of smoke emissions from packed-bed residential coal combustion devices', (April).
- Makonese, T. et al. (2017) 'Influence of fire-ignition methods and stove ventilation rates on gaseous and particle emissions from residential coal braziers', *Journal of Energy in Southern Africa*, 26(4), p. 16. <https://doi.org/10.17159/2413-3051/2016/v26i4a2089>
- Makonese, T., Masekameni, D. M. and Annegarn, H. J. (2017) 'Influence of coal properties on the performance of fixed-bed coal-burning braziers', *Journal of Energy in Southern Africa*, 28(2), pp. 40-51. <https://doi.org/10.17159/2413-3051/2017/v28i2a1374>
- Makonese, T., Meyer, J. and von Solms, S. (2019) 'Characteristics of spherical organic particles emitted from fixed-bed residential coal combustion', *Atmosphere*, 10(8), pp. 1-16. <https://doi.org/10.3390/atmos10080441>
- Makonese, T., Meyer, J. and Solms, S. Von (2019) 'Characteristics of Spherical Organic Particles Emitted from Fixed-Bed Residential Coal Combustion', pp. 1-16. <https://doi.org/10.3390/atmos10080441>
- Masekameni, D. et al. (2018) 'Size Distribution of Ultrafine Particles Generated from Residential Fixed-bed Coal Combustion in a Typical Brazier', *Aerosol and Air Quality Research*, 18(10), pp. 2618-2632. <https://doi.org/10.4209/aaqr.2018.03.0105>
- Masekameni, D., Makonese, T. and Annegarn, H. J. (2014) 'Optimisation of ventilation and ignition method for reducing emissions from coal-burning imbaulas', *Proceedings of the 22nd Conference on the Domestic Use of Energy, DUE 2014*. <https://doi.org/10.1109/DUE.2014.6827755>
- Masekameni, M. et al. (2018) 'Risk Assessment of Benzene, Toluene, Ethyl Benzene, and Xylene Concentrations from the Combustion of Coal in a Controlled Laboratory Environment', *International Journal of Environmental Research and Public Health*, 16(1), p. 95. <https://doi.org/10.3390/ijerph16010095>
- Mathis, U. et al. (2005) 'Influence of diesel engine combustion parameters on primary soot particle diameter', *Environmental Science and Technology*, 39(6), pp. 1887-1892. <https://doi.org/10.1021/es049578p>



- Mc Donald, R. and Biswas, P. (2004) 'A methodology to establish the morphology of ambient aerosols', *Journal of the Air and Waste Management Association*, 54(9), pp. 1069-1078. <https://doi.org/10.1080/10473289.2004.10470986>
- McElroy, M. W. et al. (1982) 'Size distribution of fine particles from coal combustion', *Science*, 215(4528), pp. 13-19. <https://doi.org/10.1126/science.215.4528.13>
- Meij, R. and te Winkel, H. (2007) 'The emissions of heavy metals and persistent organic pollutants from modern coal-fired power stations', *Atmospheric Environment*, 41(40), pp. 9262-9272. <https://doi.org/10.1016/j.atmosenv.2007.04.042>
- Naeher, L. P. et al. (2007) 'Woodsmoke health effects: A review', *Inhalation Toxicology*, 19(1), pp. 67-106. <https://doi.org/10.1080/08958370600985875>
- Niemi, J. V. et al. (2006) 'Changes in background aerosol composition in Finland during polluted and clean periods studied by TEM/EDX individual particle analysis', *Atmospheric Chemistry and Physics*, 6(12), pp. 5049-5066. <https://doi.org/10.5194/acp-6-5049-2006>
- Nussbaumer, T. et al. (2001) *Aerosols from biomass combustion, International Seminar by IEA Bioenergy Task.*
- Petaloti, C. et al. (2006) 'Trace elements in atmospheric particulate matter over a coal-burning power production area of western Macedonia, Greece', *Chemosphere*, 65(11), pp. 2233-2243. <https://doi.org/10.1016/j.chemosphere.2006.05.053>
- Pósfai, M. et al. (2003) 'Individual aerosol particles from biomass burning in southern Africa: 1. Compositions and size distributions of carbonaceous particles', *Journal of Geophysical Research: Atmospheres*, 108(D13), p. n/a-n/a. <https://doi.org/10.1029/2002JD002291>
- Pósfai, M. et al. (2004) 'Atmospheric tar balls: Particles from biomass and biofuel burning', *Journal of Geophysical Research: Atmospheres*, 109(D6), p. n/a-n/a. <https://doi.org/10.1029/2003JD004169>
- Schneider, J. et al. (2006) 'Mass spectrometric analysis and aerodynamic properties of various types of combustion-related aerosol particles', *International Journal of Mass Spectrometry*, 258(1-3), pp. 37-49. <https://doi.org/10.1016/j.ijms.2006.07.008>
- Shen, G. et al. (2013) 'NIH Public Access', 44(18), pp. 7157-7162. doi: 10.1021/es101313y.Emission.
- Shraim, A. et al. (2003) 'Arsenic speciation in the urine and hair of individuals exposed to airborne arsenic through coal-burning in Guizhou, PR China', *Toxicology Letters*, 137(1-2), pp. 35-48. [https://doi.org/10.1016/S0378-4274\(02\)00379-X](https://doi.org/10.1016/S0378-4274(02)00379-X)
- Silva, L. F. O. et al. (2012) 'Applied investigation on the interaction of hazardous elements binding on ultrafine and nanoparticles in Chinese anthracite-derived fly ash', *Science of the Total Environment*. Elsevier B.V., 419(July 2007), pp. 250-264. <https://doi.org/10.1016/j.scitotenv.2011.12.069>
- Smith, K. R. et al. (2014) 'Millions Dead: How Do We Know and What Does it Mean? Methods Used in the Comparative Risk Assessment of Household Air Pollution', *Ssrn*. <https://doi.org/10.1146/annurev-publhealth-032013-182356>
- Thajudeen, T., Jeon, S. and Hogan, C. J. (2015) 'The mobilities of flame synthesized aggregates/agglomerates in the transition regime', *Journal of Aerosol Science*. Elsevier, 80, pp. 45-57. <https://doi.org/10.1016/j.jaerosci.2014.11.003>
- Tissari, J. et al. (2008) 'Fine particle and gaseous emissions from normal and smouldering wood combustion in a conventional masonry heater', *Atmospheric Environment*, 42(34), pp. 7862-7873. <https://doi.org/10.1016/j.atmosenv.2008.07.019>
- Tiwari, M. et al. (2014) 'Particle size distributions of ultrafine combustion aerosols generated from household fuels', *Atmospheric Pollution Research*. Elsevier, 5(1), pp. 145-150. <https://doi.org/10.5094/APR.2014.018>
- Torvela, T. et al. (2014) 'Effect of wood combustion conditions on the morphology of freshly emitted fine particles', *Atmospheric Environment*. Elsevier Ltd, 87, pp. 65-76. <https://doi.org/10.1016/j.atmosenv.2014.01.028>
- Tóth, A. et al. (2014a) 'Atmospheric tar balls: Aged primary droplets from biomass burning?', *Atmospheric Chemistry and Physics*, 14(13), pp. 6669-6675. <https://doi.org/10.5194/acp-14-6669-2014>
- Tóth, A. et al. (2014b) 'Atmospheric tar balls: Aged primary droplets from biomass burning?', *Atmospheric Chemistry and Physics*, 14(13), pp. 6669-6675. <https://doi.org/10.5194/acp-14-6669-2014>
- Vanhaecke, Frank, et al. (1992). 'The use of internal standards in ICP-MS', *Talanta*, 39(7), pp. 737-742. [https://doi.org/10.1016/0039-9140\(92\)80088-U](https://doi.org/10.1016/0039-9140(92)80088-U)
- Wang, A. Q. C. and Luo, B. Y. H. (2009) 'Application SEM to analysis formation characteristic of soot aerosol emitted from lump-coal combustion in fixed-bed', *Asia-Pacific Power and Energy Engineering Conference, APPEEC*, pp. 2-5. <https://doi.org/10.1109/APPEEC.2009.4918190>
- Wang, W. et al. (2018) 'Characteristics of Individual Particles Emitted from an Experimental Burning Chamber with the Coal from Lung Cancer Area of Xuanwei, China', *Aerosol and Air Quality Research*, pp. 1-9. <https://doi.org/10.4209/aaqr.2018.05.0187>
- Wilkinson, P. et al. (2009) 'Public health benefits of strategies to reduce greenhouse-gas emissions: household energy', *The*

Lancet, 374(9705), pp. 1917-1929. [https://doi.org/10.1016/S0140-6736\(09\)61713-X](https://doi.org/10.1016/S0140-6736(09)61713-X)

Zhang, Zou, X., et al. (2018) 'Decoupling greenhouse gas emissions from crop production: A case study in the Heilongjiang land reclamation area, China', *Energies*, 11(6). <https://doi.org/10.3390/en11061480>

Zhang, Liu, C., et al. (2018) 'Morphology and property investigation of primary particulate matter particles from different sources', *Nano Research*, 11(6), pp. 3182-3192. <https://doi.org/10.1007/s12274-017-1724-y>

Zhang, H. et al. (2012) 'Chemical and size characterization of particles emitted from the burning of coal and wood in rural households in Guizhou, China', *Atmospheric Environment*. Elsevier Ltd, 51, pp. 94-99. <https://doi.org/10.1016/j.atmosenv.2012.01.042>

Zhang, Y. and Tao, S. (2009) 'Global atmospheric emission inventory of polycyclic aromatic hydrocarbons (PAHs) for 2004', *Atmospheric Environment*. Elsevier Ltd, 43(4), pp. 812-819. <https://doi.org/10.1016/j.atmosenv.2008.10.050>

Zhou, M. et al. (2015) 'Smog episodes, fine particulate pollution and mortality in China', *Environmental Research*. Elsevier, 136, pp. 396-404. <https://doi.org/10.1016/j.envres.2014.09.038>

Zhou, W. et al. (2016) 'Evolution of submicrometer organic aerosols during a complete residential coal combustion process', *Environmental Science and Technology*, 50(14), pp. 7861-7869. <https://doi.org/10.1021/acs.est.6b00075>